IEEE Access
Multidisciplinary ⋮ Rapid Review ⋮ Open Access Journal

Received June 16, 2020, accepted June 30, 2020, date of publication July 9, 2020, date of current version July 22, 2020.

Digital Object Identifier 10.1109/ACCESS.2020.3008234

High Gain Antenna Miniaturization With Parasitic Lens

DUY-NINH DANG AND CHULHUN SEO, (Senior Member, IEEE)
Department of Information and Telecommunication Engineering, Soongsil University, Seoul 06978, South Korea

Corresponding author: Chulhun Seo (chulhun@ssu.ac.kr)

This work was supported by the National Research Foundation of Korea (NRF) Grant funded by the Korean Government Minister of Science, ICT and Future Planning (MSIP) under Grant NRF-2017R1A5A101 5596.

ABSTRACT The scenario of using a spatially distributed antenna for miniaturized applications is presented in this work. A model of lens antenna with a low profile, compact, and high focusing superstrate, which exquisitely combines the conventional lens and resonant cavity superstrates, is proposed. Based on this model, the parasitic lens superstrate is introduced with high performance and simple configuration. The parasitic lens includes a low dielectric substrate and high resonant parasitic elements. By manipulating the surface currents of parasitic elements concentrating at center region of superstrate, the focusing effect is obtained. A prototype of the parasitic lens antenna was implemented with the source and parasitic superstrate's lateral dimensions of $0.5\lambda_0 \times 0.5\lambda_0$ and $\lambda_0 \times \lambda_0$, respectively, and the profile of $0.54\lambda_0$. The peak gain is 10 dBi, corresponding to the enhancement of 5 dB. The measured results perspicuously demonstrate the efficiency of the compact parasitic lens.

INDEX TERMS Antenna miniaturization, compact, gain enhancement, high focusing, parasitic lens.

I. INTRODUCTION

Due to the avalanche of 5G handset [1]–[6], wearable [7]–[13], and implant wireless devices [14]–[19], the needs for antenna miniaturization are increasingly extended. However, the reducing dimension of antenna causes the restriction on its performance including bandwidth, radiation efficiency, and especially for gain [20]–[22]. The antenna miniaturization inherently has a narrow radiation area that broadens the divergence of the emitted wave results of the low directivity and gain. Relatively, the gain enhancement method is classified into two kinds, planar and spatial structures. The planar structure such as antenna array enhances directivity by adding more radiation elements [2], [3]. However, this technique significantly broadens the lateral size of antenna which is restricted in some applications such as bio-implant or highly integrated circuit. Meanwhile, the spatially distributed antenna delicately manipulates 3D structure to enhance directivity of an excited source [17], [19]. Even though it is a prospective approach, current works have not obtained a significant enhancement. These works all set up parasitic elements in reactive region of sourced antenna to reduce the profile of structure. However, this is the main reason of the low enhancement in comparison to the high profile antenna.

Resonant cavity and lens structures are two common types of high gain spatially distributed antenna which all use the superstrate to enhance the directivity of an excited source. In the case of resonant cavity antenna (RCA), the superstrate is configured as a partially reflecting surface [23]–[28] while the ground of the feed source is a perfectly reflecting surface. The gain enhancement is proportional to the reflection between two reflecting surfaces. Consequently, the dimension of the sourced antenna must be as large as the superstrate, which prevents it from many applications. Compact and high gain structures have been proposed but not enough for miniatured applications [28]. On another hand, the lens antenna installs the superstrate as a high focusing lens in front of a small antenna element as a focal point [29]–[31]. Currently, metamaterial/metasurface is a popular superstrate of the lens antenna due to its high performance and ability of easily combining with printed antennas [32]–[41]. The meta-lens is constituted by meta-cells which are configured with high transmission and zero/low/gradient-refractive-indexes or phase gradient. Meta-lens antenna allows the sourced antenna in compact size; however, to achieve the high gain, the superstrate is paid by large lateral dimension [32], [35], [40], high profile [32], [39], [40],

The associate editor coordinating the review of this manuscript and approving it for publication was Yingsong Li.

multilayer [32], [39]–[41], or complex structure [32], [37], [39], [40]. The compact and high gain meta-lens antennas have also been propounded. However, these structures present an issue that the sourced antenna has the same lateral size with the superstrate due to the large ground [37], [39]–[41]. This configuration diminishes the focusing and focal behaviors of the superstrate and feed source, respectively. In addition, the role of ground and its interaction with the superstrate have not been considered thoroughly.

In this work, a scenario of using the spatially distributed structure is proposed to significantly improve the performance of antenna miniaturization. The capability of this scenario is discussed in two specific applications including biomedical implant and highly integrated circuit. Based on this scenario, a model of the spatially distributed antenna with a compact superstrate is proposed, which manipulates the reflecting and transmitting characteristics of the superstrate to obtain the high focusing. The theory of field regions applied to the small sourced antenna is the fundamental basis of the analysis. Finally, a high gain and compact parasitic lens antenna is introduced. The novel parasitic lens superstrate is low profile, compact, and high focusing. The simplicity as an inherent advantage of parasitic structure is also expressed.

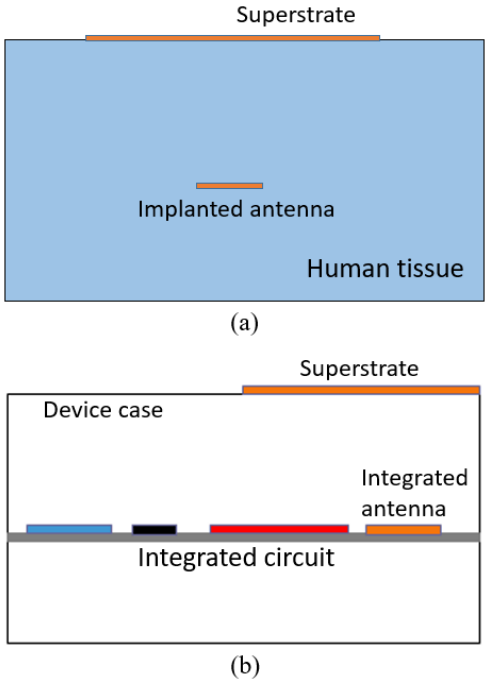

FIGURE 1. Scenario of spatially distributed antenna miniaturizations. (a) Bio-implant application. (b) Highly integrated circuit application.

II. DESIGN ANALYSIS

A. SCENARIO OF A SPATIALLY DISTRIBUTED ANTENNA MINIATURIZATION

In a number of applications, the lateral size is required to be strictly restricted, but the spatial dimension is not since it is a prerequisite for superstrate installation. However, to effectively deploy a high gain spatially distributed antenna, the free spatial dimension must be larger than the reactive range of the sourced antenna. The feasibility of this scenario is assessed through two applications, biomedical implant and highly integrated circuit, as illustrated in Fig. 1. In bio-implant applications, the space between the implanted chip antenna and the outer of the body facilitates the installation of a superstrate. The range of this space is from mm to a few cm, depending on the position of the implanted substance. Within the bounds of the operating frequency from 10 MHz to a few GHz [42], this range allows the setup of the superstrate outside the reactive region of the sourced antenna. Similarly, it is possible for setting the superstrate on the case of an electronic device to enhance the antenna which is embedded inside the integrated circuit. The feasibility of this structure for ultra-thin devices such as mobile-phone can exist when the mobile frequency lifts on the millimeter-wave band. At this band, the physical distance between the integrated antenna and mobile case, a few mm, can meet the electrical gap condition of the superstrate. To accommodate this scenario, the ideal spatially distributed antenna must satisfy the following conditions:

1) Small feeding antenna (receiving antenna in case of receiver).
2) Compact superstrate.
3) Low or wide range of profile.
4) High directivity (focusing) and radiation efficiency.
5) High isolation, low side-lobe and back-lobe levels.

In this work, a low profile, compact, and high focusing superstrate takes precedence over others.

B. FIELD REGIONS OF AN ELECTRICALLY SHORT ANTENNA

With the objectives of high focusing and low profile, the superstrate should be confined in the radiating near-field region of the source. However, the boundary among the field regions of an antenna is vague, especially for an electrically short antenna [44]. This work introduces an approach to define the field regions of the electrically short antenna with quasi-spherical emitted waves, as shown in Fig. 2(a). The ranges of the reactive and radiating near fields are R_1 and R_2, respectively. The range of radiating far-field is from its boundary with the radiating near-field to the infinity. The reactive region is approximately $\lambda_0/2\pi$, where λ_0 is the air wavelength emitted by the source. Meanwhile, the boundary between the radiating near-field and far-field is determined on basis of the angular field distribution's dependence on the distance from the source. In the radiating near-field, the field distribution has a quasi-spherical waveform, but the angular decreases far from the source. In the far-field, the field distribution has a pattern closing as a plane wave in which its angular field distribution is independent of the distance. Due to the broad divergence of emitted waves caused by the small radiation area, the radiating near-field region of the short antenna is wider than the long one. Figure 3 plots the field

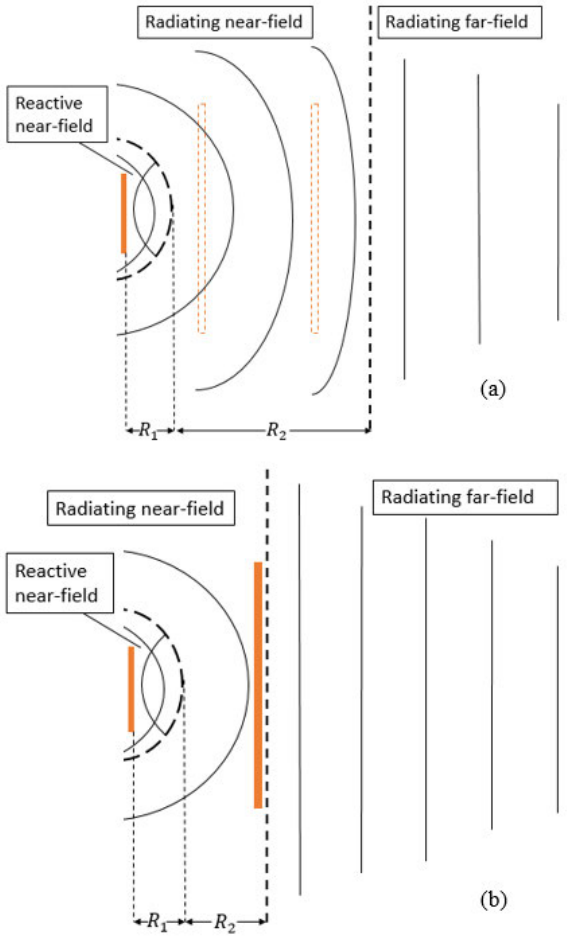

FIGURE 2. Field regions of an electrically short antenna with quasi-spherical emitted waves: (a) Without superstrate. (b) With superstrate.

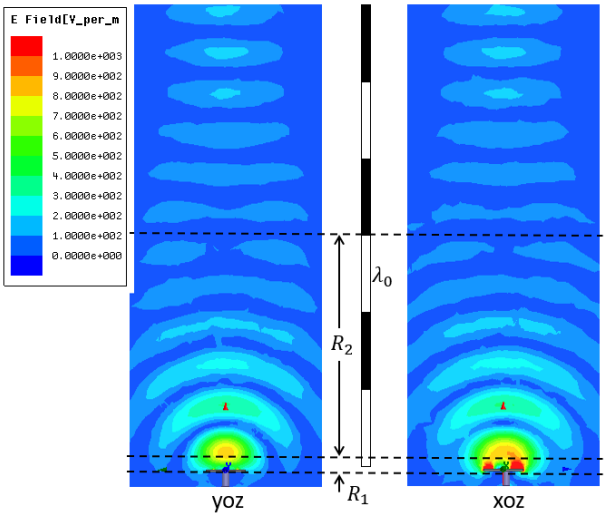

FIGURE 3. Plot of the field regions of a small microstrip patch antenna.

regions of a conventional square microstrip patch antenna with its length of $\lambda_0/2$. The radiating near-field range is up to $R_2 \approx 3\lambda_0$ which is much wider than the range calculated by the common formula of $2D^2/\lambda_0$ ($R_2 \approx \lambda_0/2$), where D is the largest dimension of the source.

Based on this approach, the function of the lens superstrate is recognized in another aspect. The lens superstrate typically has a function of transforming the quasi-spherical wave of the source into the uniform plane wave which is more directive than the quasi-spherical wave. By observing the field regions' aspect, the lens superstrate effectively reduces the range of the radiating near-field region, as illustrated in Fig. 2(b). Ideally, if the superstrate has enough low profile and perfect transforming function, the radiating near-field region may not exist. Reduction in radiating near-field has a considerable significance for compact ranges in various applications such as antenna pattern measurements, gain comparisons, boresight measurements, radar reflectivity measurements, and the illumination of animals and humans to study biological effects of microwave radiation [44].

C. A MODEL OF LENS ANTENNA WITH COMPACT SUPERSTRATE

As shown in Fig. 2 and 3, the field distribution near the source has a high intensity and wide angular variation. The former behavior allows a compact superstrate which makes a significant contribution to the far-field performance of the antenna while the latter is a real challenge. The manipulation of many incident waves with different angles reaching to a narrow area is hardly efficient even with infinitesimal structures such as metamaterials. Commonly, a meta-unit-cell is configured to adapt a small range of the incident angle, and the effectiveness is only obtained with enough number of cells. As a result, current meta-lens shows strong enhancement with the high profile and large dimension, but the performance is quickly dropped in the opposite case. On another hand, the RCA which is made from two parallel reflecting surfaces, the ground of the source as a perfectly reflecting surface and the thin superstrate as a partially reflecting surface, is capable of significantly improving the directivity of the source with a compact microstrip superstrate. The incident waves can pass through the cavity only when they are in resonance with it. This effect guarantees every leaky-wave from the cavity is obtained in phase with the source. In addition, the high resonance of microstrip elements attracts the incident waves to focus on themself, which reduces the range of the incident angle. This focus is repeated with the partially reflected waves which are generated by two reflecting surfaces. As a result, the high gain broadside radiation pattern is obtained with the compact superstrate. Relatively, the restriction of the RCA in comparison to the lens antenna is the large lateral size of the source due to its ground as one of two reflecting surfaces. However, in the case of compact superstrate as mentioned above, establishing a part of the superstrate as a partially reflecting surface is appreciable.

A novel model of the lens antenna with a compact superstrate is proposed in this work, as shown in Fig. 4. The superstrate is divided into two parts, high transmission and reflection. The highly reflecting part at the center of the

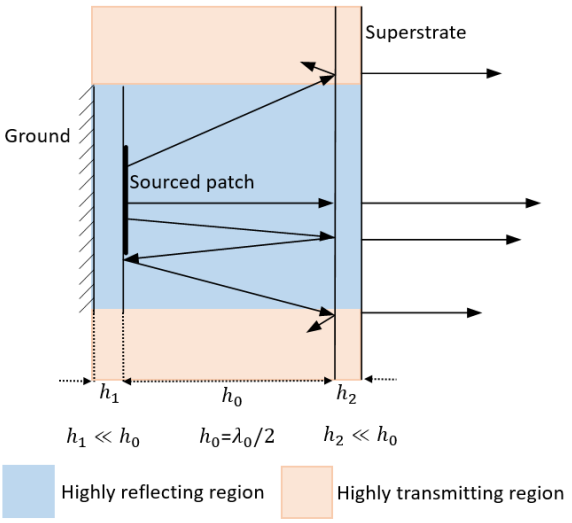

FIGURE 4. Proposed model of a lens antenna with a compact superstrate.

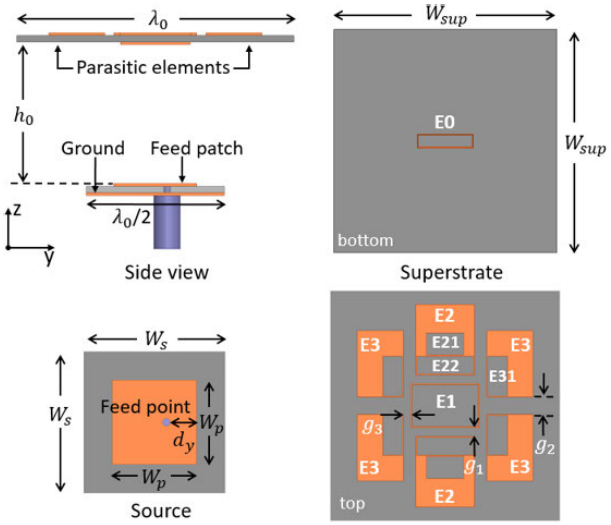

W_{sup}	W_s	W_p	h_0	d_y	g_1	g_2	g_3
52	26	15.5	26	2.2	2	4	2

Parameter	E0	E1	E2	Subtract		E3	Subtract
				E21	E22		E31
Width	13	15.5	13.3	8.5	12.9	10.5	4.5
Length	3.2	10	16	5	4	15	9

FIGURE 5. Proposed parasitic lens antenna and its parameters (mm).

superstrate combines with the ground as a pair of reflecting surfaces. The outside region of the superstrate is configured as the conventional lens antenna with high transmission and low reflection coefficients. The contribution of each region to the antenna's performance depends on their dimensional relation. The reflecting region expands when the source's size is large, and vice versa. The gap between the source and the superstrate is $\lambda_0/2$ to satisfy the resonant condition of the RCA. The thickness of the two substrates is much smaller than their gap to compact design and be considered as planes.

The multi-function of proposed superstrate leads to the need of a non-periodic microstrip structure. For the RCA, the hybrid-parasitic superstrate has been introduced with high gain and compact size [28]. This structure is also much simpler than others such as frequency selective surface or metamaterial that is valid to reduce cost and design time. Even though the parasitic structure is a good candidate to the compact RCA, it has not been applied for the lens antenna.

III. PROPOSED PARASITIC LENS ANTENNA

This work proposes a parasitic lens superstrate with objectives of high gain, compact size, and simple structure, as shown in Fig. 5. All designed component parameters are also presented in the unit of mm. The operating frequency is 5.8 GHz. The source is a square conventional microstrip patch antenna with a width of $\lambda_0/2$. Its narrow ground helps to decrease the lateral size but causes a reduction in the realized gain and an increase in the back-lobe level. The superstrate has a width of λ_0 and is suspended in the air at $h_0 = \lambda_0/2$. The parasitic elements are etched on both sides of the superstrate with one rectangular ring on the bottom and 7 hybrid elements on top. The categorization of elements (E0, E1, E2, and E3) and the arrangement of the hybrid structure are inherited the RCA as in [28], but the configuration is different. Both source and superstrate use the same substrate of Taconic TLY with the dielectric constant of 2.2 and the thickness of 1.2 mm ($0.02\lambda_0$). The aim of using low dielectric constant substrate is to reduce the superstrate's reflection which will be dominantly controlled by the parasitic elements.

To explain the proposed parasitic array, the study on fundamental single parasitic elements is prior presented. Figure 6 illustrates Poynting vectors of two single parasitic elements, parasitic patch and ring. Two elements have the same resonant frequency of 5.8 GHz, but the ring is more compact than the other. The Poynting vectors indicate that the reflection and the self-resonance of the ring are larger than those of the patch which has a good transmission and low reflection. Their co-polarization radiation patterns associate the reflection and transmission effects with the antenna's performance, as illustrated in Fig. 7. The ring antenna has higher realized gain and back-lobe level than the patch one. Especially, when the ring is located at the bottom of the superstrate, the highest gain and back-lobe level are presented due to the strong reflection.

The expression of basic parasitic elements essentially explains the parasitic lens's configuration. Two parasitic rings, E0 and E1, at the center on both sides of the superstrate are to enhance the reflection with the source. The others are divided into two groups, E2 and E3. These elements are subtracted where is adjacent to the center ring, especially for E2; two subtractions are conducted. By the subtraction, each element is divided into two parts, ring part adjacent to the center ring and patch one at the outside. This configuration enhances the reflection at the center and reduces the same

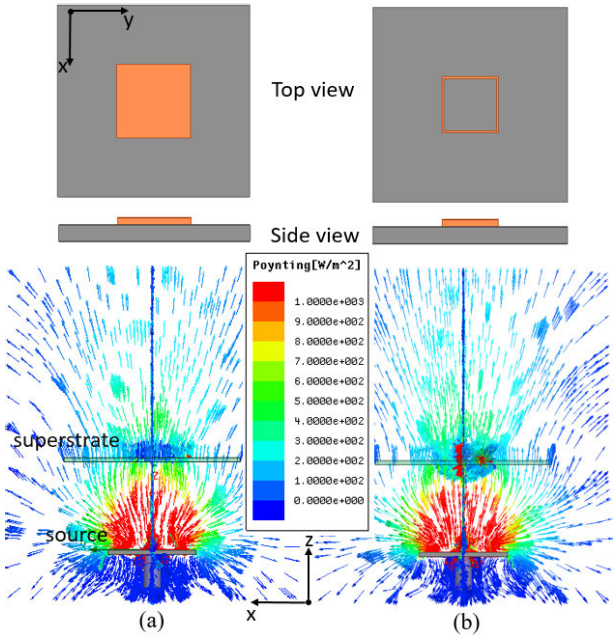

FIGURE 6. Poynting vectors of various single parasitic elements: (a) Parasitic patch. (b) Parasitic ring.

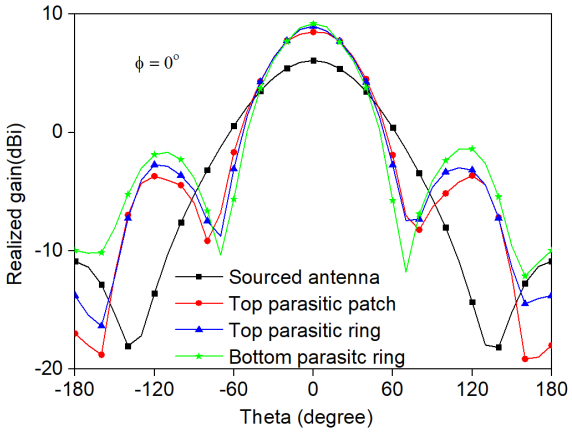

FIGURE 7. Radiation patterns of various single parasitic elements.

at the outside of the superstrate as the intension. The meaning of this work is distinctly plotted in Fig. 8. The surface currents of the proposed parasitic lens are concentrated at the center of the superstrate, which is totally different from the uniform currents of the periodic parasitic patches. The proposed Poynting vectors illustrate strong reflection at the center, low reflection and high transmission at the outside. Hence, the proposed antenna shows a stronger focus than the periodic one.

The re-distribution of the surface currents on E2 and E3 is conducted by two essential effects, skin and proximity effects. Due to the skin effect, the E-field tends to concentrate at the edge of the parasitic patch, which also explains the equivalence of the parasitic ring and patch. On another hand, the proximity effect induces the currents to concentrate at

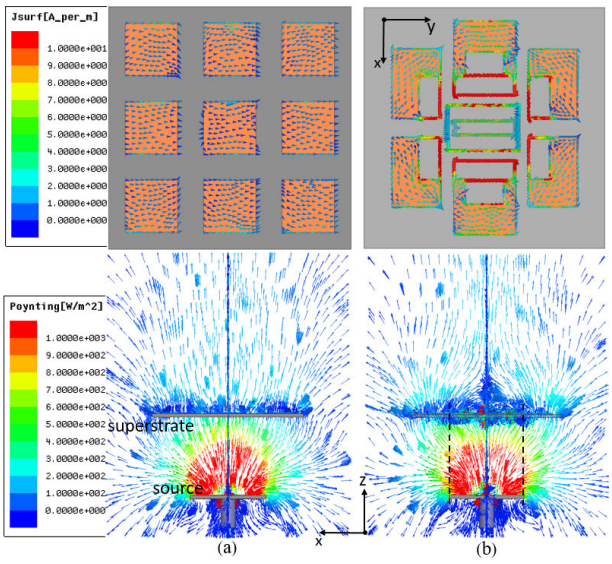

FIGURE 8. Surface currents and Poynting vector expressions: (a) Periodic parasitic patches. (b) Proposed parasitic lens.

the adjacent region between elements. Deliberately, this work reduces the distance between the center ring and the others to increase their proximity effect. Because the increasing proximity effect causes the increment of the self-resonance, the size of these parasitic components should be enlarged to calibrate the resonant frequency. Therefore, the subtraction of E2 and E3 not only handles the reflection and transmission of the superstrate through the surface currents of parasitic elements but also reduces the size of parasitic patches.

For the purpose of comparing various parasitic structures, Figure 9 plots their realized gain versus the size of the source. The periodic rings have high performance with the large ground due to high reflection, but their performance is quickly dropped with the small ground. In contrast, the periodic patches have higher gain with the small source, but lower gain with the large one. Overall, the novel parasitic lens

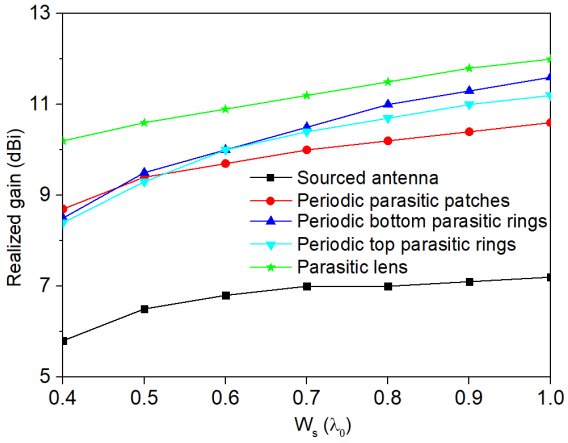

FIGURE 9. Realized gain of various antenna versus lateral size of the source.

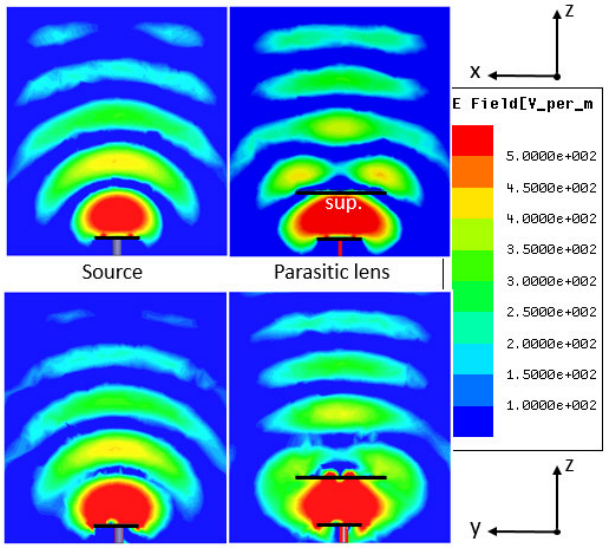

FIGURE 10. Quasi-spherical wave to plane wave transformation.

presents a considerable improvement in both cases, especially for the small source. As the featured characteristic of the lens superstrate, the conversion from quasi-spherical to plane waves in both orthogonal planes is shown in Fig. 10. The main difference between the proposed lens and the conventional meta-lens could be easily realized that the emitted E-field from the source highly focuses at the center of the superstrate. The strong focus of parasitic lens antenna is clearly indicated at the far-field region.

IV. RESULTS AND DISCUSSION

To validate the proposed antenna, its prototype is fabricated, as shown in Fig. 11. To align with the superstrate, the source is covered by an aligning structure that does not affect the antenna's performance. Measurements of reflection coefficient and radiation pattern are conducted, as shown in Fig. 12. The reflection coefficient S_{11} is measured by using HP 8719D vector network analyzer with covering frequencies from 50 MHz to 13.5 GHz. The radiation characteristics are measured in the microwave anechoic chamber with the range from 600 MHz to 6 GHz. The prototype is placed in the far-field of transmitting antenna and mounted on a position that can be freely rotated. To measure the radiation pattern as a function of angle, the prototype is rotated so that the transmitting antenna illuminates the prototype from different angles.

The measured reflection coefficient and realized gain versus the operating frequency are shown in Fig. 13. Due to the location near the reactive region of the source and the high reflection from the center of the superstrate, the impedance of the source is influenced, which increases its resonant frequency. Furthermore, the soldering in the fabrication causes the shift-up of the source's resonant frequency. Consequently, the resonances of the source in simulation and measurement are 5.9 GHz and 5.95 GHz, respectively. Because of this

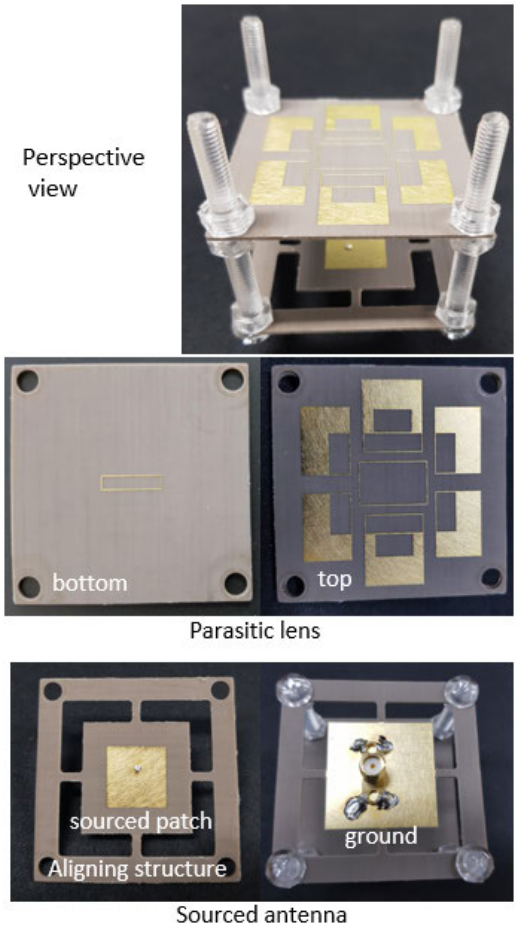

FIGURE 11. Prototype of proposed antenna.

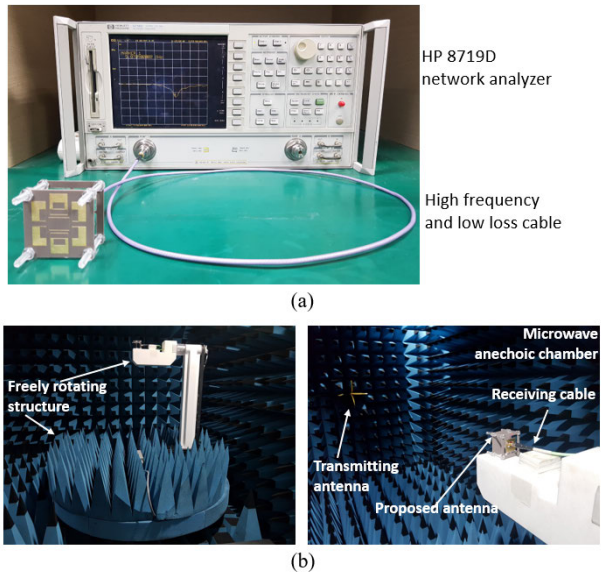

FIGURE 12. Measurements setup: (a) Reflection coefficient. (b) Radiation pattern.

shift-up, the lens antenna resonance also moves from 5.8 GHz in simulation to 5.87 GHz in measurement. The simulated and measured realized gain of the proposed antenna is 10.6 dBi

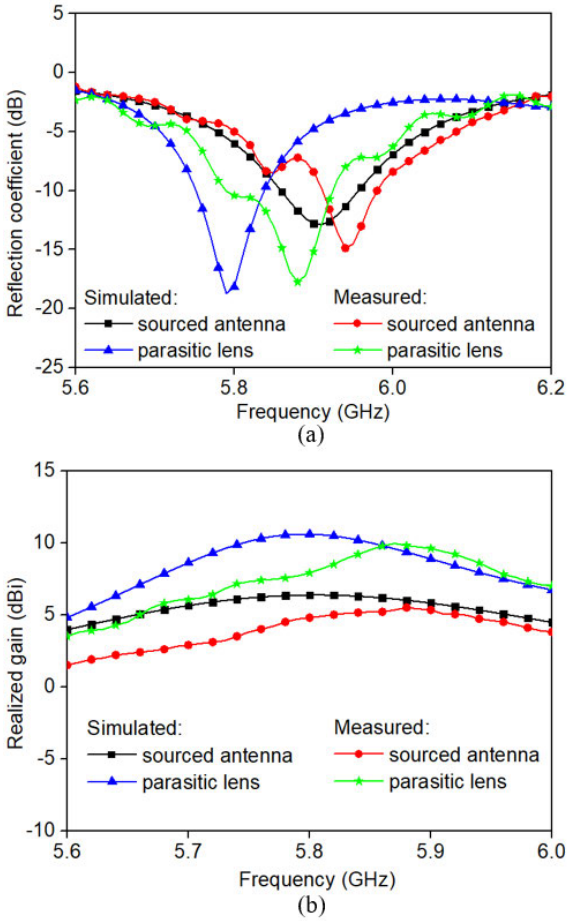

FIGURE 13. Measured results versus frequency: (a) Reflection coefficient. (b) Realized gain.

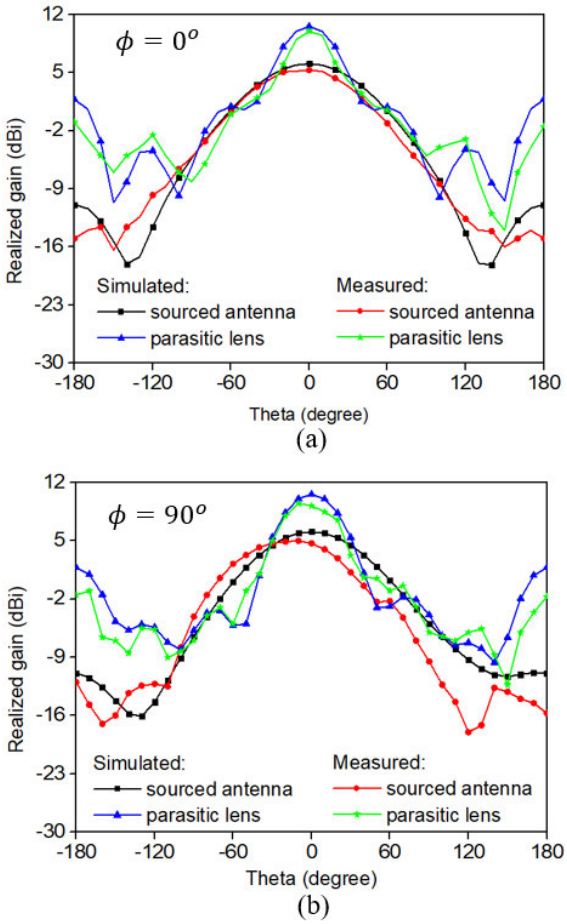

FIGURE 14. Measured realized gains with two principal planes: (a)$\phi = 0^o$. (b)$\phi = 90^o$.

at 5.8 GHz in simulation and 10 dBi at 5.87 GHz in measurement. In both cases, the gain enhancements are 5 dB. The peak gains at 5.87 GHz with the co-polarization radiation pattern in two principal planes ($\phi = 0^o$ and $\phi = 90^o$) are plotted in Fig. 14. The corresponding 3D radiation pattern measurement is shown in Fig. 15. The lens antenna's beamwidth is much smaller than the source's due to the high focusing effect. The side-lobe level is almost neglected; however, due to the small ground and the high reflection from the center of the superstrate, the back-lobe level is quite high, approximately 12 dB. Nevertheless, this parameter can be improved by the trade-off with the realized gain or using other substrates with the high dielectric constant to enlarge the area of the ground.

The contribution of this work is demonstrated by a comparison table which summarizes current works of high gain spatially distributed antennas, as listed in Table 1. The proposed antenna achieves a good gain enhancement with compactness and simplicity. In comparison with the RCA, the small source of the proposed antenna exhibits as the most advantage that allows it to adapt various miniatured applications. In addition, compared to the meta-lens antenna, the proposed antenna

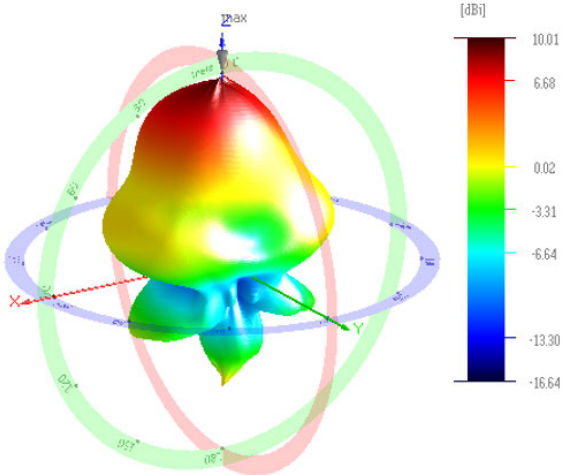

FIGURE 15. 3D radiation pattern measurement.

possesses the parasitic lens which displays as a low profile, simpler and more compact structure than the meta-lens. Simplicity, with only single superstrate and eight microstrip elements, is the most outstanding characteristic of the parasitic lens which remarkably reduces the cost and design time.

TABLE 1. Comparison with a few recently proposed RCA and meta-lens antennas.

Year/Ref.	Dimension			Gain		Superstrate	
	Feed source($\lambda_0 \times \lambda_0$)	Superstrate($\lambda_0 \times \lambda_0$)	Profile(λ_0)	Peak gain (dBi)	Enhancement(dB)	Type	Number of layers/cells
2015 [24]	1.93×1.93	1.93×1.93	0.63	13.80	5.30	RCA/HDS	1/0
2017 [25]	2.75×2.75	2.75×2.75	0.56	16.00	8.20	RCA/HDS	1/0
2017 [26]	2.21×2.21	2.21×2.21	0.58	16.35	12.50	RCA/MM	125
2019 [27]	1.95×1.95	1.95×1.95	0.58	15.75	N/A	RCA/FSS	1/99
2019 [28]	1.35×1.35	1.35×1.35	0.63	15.80	4.50	RCA/HPR	1/7
2015 [32]	0.40×0.40	4.34×4.34	1.80	18.50	11.6	Meta-lens	4/169
2019 [35]	2.93×2.93	3.30×3.30	0.55	18.60	11.00	Meta-lens	1/76
2016 [37]	1.00×1.00	1.00×1.00	0.50	10.70	5.50	Meta-lens	1/256
2018 [39]	1.54×1.54	1.54×1.54	0.83	14.50	5.00	Meta-lens	2/120
2019 [40]	4.42×4.42	4.42×4.42	1.10	19.40	11.30	Meta-lens	4/676
2019 [41]	1.80×1.80	1.80×1.80	0.56	15.49	10.70	Meta-lens	3/48
This work	0.50×0.50	1.00×1.00	0.54	10.00	5.00	Parasitic-lens	1/8

λ_0: Air wavelength N/A: Not available HDS: Homogeneous dielectric superstrate
FSS: Frequency selective surface MM slab: Metamaterial slab. HPR: Hybrid parasitic ring

V. CONCLUSION

This work presents a scenario of using spatially distributed antenna miniaturization in various applications, i.e., biomedical implant and highly integrated circuit. Low profile, compact, and high focusing superstrate is defined for this scenario. Based on the analysis of the small source's field regions, a model of high gain spatially distributed antenna with a compact superstrate is proposed. The model is a sophisticated combination of two popular superstrates, partial reflection and lens. The parasitic lens is then introduced as a high focusing, simple, low profile, and compact structure. By manipulating the surface currents of parasitic elements, the novel lens has a strong reflection at the central region, strong transmission and weak reflection at the outside. In consequence, the high focusing lens is obtained as the intention of the proposed model. A prototype of the parasitic lens antenna was implemented. The lateral dimensions of the source and the superstrate are $0.5\lambda_0 \times 0.5\lambda_0$ and $\lambda_0 \times \lambda_0$, respectively. The profile (center to center distance) of the antenna is $0.54\lambda_0$. The peak gain is 10 dBi, corresponding to the enhancement of 5 dB. A comparison of the proposed antenna's performance with the designs' in the literature is illustrated to prove the contribution of this work. Compactness and simplicity are two outstanding features of the parasitic lens in comparison to the conventional meta-lens.

REFERENCES

[1] K. Ming Mak, H. Wah Lai, K. Man Luk, and C. Hou Chan, "Circularly polarized patch antenna for future 5G mobile phones," *IEEE Access*, vol. 2, pp. 1521–1529, 2014.

[2] P. Liu, X. Zhu, Z. H. Jiang, Y. Zhang, H. Tang, and W. Hong, "A compact single-layer Q-band tapered slot antenna array with phase-shifting inductive windows for endfire patterns," *IEEE Trans. Antennas Propag.*, vol. 67, no. 1, pp. 169–178, Jan. 2019.

[3] S. Zhu, H. Liu, and P. Wen, "A new method for achieving miniaturization and gain enhancement of Vivaldi antenna array based on anisotropic metasurface," *IEEE Trans. Antennas Propag.*, vol. 67, no. 3, pp. 1952–1956, Mar. 2019.

[4] X. Shen, Y. Liu, L. Zhao, G.-L. Huang, X. Shi, and Q. Huang, "A miniaturized microstrip antenna array at 5G millimeter-wave band," *IEEE Antennas Wireless Propag. Lett.*, vol. 18, no. 8, pp. 1671–1675, Aug. 2019.

[5] M. Aboualalaa, I. Mansour, H. Elsadek, A. B. Abdel-Rahman, A. Allam, M. Abo-Zahhad, K. Yoshitomi, and R. K. Pokharel, "Independent matching dual-band compact quarter-wave half-slot antenna for millimeter-wave applications," *IEEE Access*, vol. 7, pp. 130782–130790, 2019.

[6] R. Yazdani, M. Yousefi, H. Aliakbarian, H. Oraizi, and G. A. E. Vandenbosch, "Miniaturized triple-band highly transparent antenna," *IEEE Trans. Antennas Propag.*, vol. 68, no. 2, pp. 712–718, Feb. 2020.

[7] S. Yan, P. J. Soh, and G. A. E. Vandenbosch, "Compact all-textile dual-band antenna loaded with metamaterial-inspired structure," *IEEE Antennas Wireless Propag. Lett.*, vol. 14, pp. 1486–1489, 2015.

[8] S. Agneessens, S. Lemey, T. Vervust, and H. Rogier, "Wearable, small, and robust: The circular quarter-mode textile antenna," *IEEE Antennas Wireless Propag. Lett.*, vol. 14, pp. 1482–1485, 2015.

[9] S. Genovesi, F. Costa, F. Fanciulli, and A. Monorchio, "Wearable inkjet-printed wideband antenna by using miniaturized AMC for sub-GHz applications," *IEEE Antennas Wireless Propag. Lett.*, vol. 15, pp. 1927–1930, 2016.

[10] M. E. Lajevardi and M. Kamyab, "Ultraminiaturized metamaterial-inspired SIW textile antenna for off-body applications," *IEEE Antennas Wireless Propag. Lett.*, vol. 16, pp. 3155–3158, 2017.

[11] J. Zhang, S. Yan, and G. A. E. Vandenbosch, "A miniature feeding network for aperture-coupled wearable antennas," *IEEE Trans. Antennas Propag.*, vol. 65, no. 5, pp. 2650–2654, May 2017.

[12] A. Y. I. Ashyap, Z. Zainal Abidin, S. H. Dahlan, H. A. Majid, A. M. A. Waddah, M. R. Kamarudin, G. A. Oguntala, R. A. Abd-Alhameed, and J. M. Noras, "Inverted E-shaped wearable textile antenna for medical applications," *IEEE Access*, vol. 6, pp. 35214–35222, 2018.

[13] G.-P. Gao, C. Yang, B. Hu, R.-F. Zhang, and S.-F. Wang, "A wearable PIFA with an all-textile metasurface for 5 GHz WBAN applications," *IEEE Antennas Wireless Propag. Lett.*, vol. 18, no. 2, pp. 288–292, Feb. 2019.

[14] H. Bahrami, S. A. Mirbozorgi, R. Ameli, L. A. Rusch, and B. Gosselin, "Flexible, polarization-diverse UWB antennas for implantable neural recording systems," *IEEE Trans. Biomed. Circuits Syst.*, vol. 10, no. 1, pp. 38–48, Feb. 2016.

[15] V. T. Nguyen and C. W. Jung, "Radiation-pattern reconfigurable antenna for medical implants in MedRadio band," *IEEE Antennas Wireless Propag. Lett.*, vol. 15, pp. 106–109, 2016.

[16] C. W. L. Lee, A. Kiourti, and J. L. Volakis, "Miniaturized fully passive brain implant for wireless neuropotential acquisition," *IEEE Antennas Wireless Propag. Lett.*, vol. 16, pp. 645–648, 2017.

[17] S. Ma, L. Sydanheimo, L. Ukkonen, and T. Bjorninen, "Split-ring resonator antenna system with cortical implant and head-worn parts for effective far-field implant communications," *IEEE Antennas Wireless Propag. Lett.*, vol. 17, no. 4, pp. 710–713, Apr. 2018.

[18] V. Kaim, B. K. Kanaujia, and K. Rambabu, "Design of a miniaturised broadband 3×3 mm antenna for intraocular retinal prosthesis application," *Electron. Lett.*, vol. 54, no. 20, pp. 1150–1152, Oct. 2018.

[19] H. M. Bernety, R. D. Puckett, D. Schurig, and C. Furse, "Comparison of passive 2-D and 3-D ring arrays for medical telemetry focusing," *IEEE Antennas Wireless Propag. Lett.*, vol. 18, no. 6, pp. 1189–1193, Jun. 2019.

[20] M. Fallahpour and R. Zoughi, "Antenna miniaturization techniques: A review of topology- and material-based methods," *IEEE Antennas Propag. Mag.*, vol. 60, no. 1, pp. 38–50, Feb. 2018.
[21] A. Kiourti, "RFID antennas for body-area applications: From wearables to implants," *IEEE Antennas Propag. Mag.*, vol. 60, no. 5, pp. 14–25, Oct. 2018.
[22] R. Karim, A. Iftikhar, B. Ijaz, and I. Ben Mabrouk, "The potentials, challenges, and future directions of On-Chip-Antennas for emerging wireless Applications—A comprehensive survey," *IEEE Access*, vol. 7, pp. 173897–173934, 2019.
[23] G. V. Trentini, "Partially reflecting sheet arrays," *IRE Trans. Antennas Propag.*, vol. 4, no. 4, pp. 666–671, Oct. 1956.
[24] X. Chen, Z. Luo, Z. Zheng, P. Feng, and K. Huang, "Effective reflective characteristics of superstrates and their effects on the resonant cavity antenna," *IEEE Trans. Antennas Propag.*, vol. 63, no. 4, pp. 1572–1580, Apr. 2015.
[25] L.-Y. Ji, P.-Y. Qin, and Y. J. Guo, "Wideband Fabry–Pérot cavity antenna with a shaped ground plane," *IEEE Access*, vol. 6, pp. 2291–2297, 2018.
[26] A. K. Singh, M. P. Abegaonkar, and S. K. Koul, "High-gain and high-aperture-efficiency cavity resonator antenna using metamaterial superstrate," *IEEE Antennas Wireless Propag. Lett.*, vol. 16, pp. 2388–2391, 2017.
[27] A. Lalbakhsh, M. U. Afzal, K. P. Esselle, S. L. Smith, and B. A. Zeb, "Single-dielectric wideband partially reflecting surface with variable reflection components for realization of a compact high-gain resonant cavity antenna," *IEEE Trans. Antennas Propag.*, vol. 67, no. 3, pp. 1916–1921, Mar. 2019.
[28] D.-N. Dang and C. Seo, "Compact high gain resonant cavity antenna with via hole feed patch and hybrid parasitic ring superstrate," *IEEE Access*, vol. 7, pp. 161963–161974, 2019.
[29] D. McGrath, "Planar three-dimensional constrained lenses," *IEEE Trans. Antennas Propag.*, vol. AP-34, no. 1, pp. 46–50, Jan. 1986.
[30] D. M. Pozar, "Flat lens antenna concept using aperture coupled microstrip patches," *Electron. Lett.*, vol. 32, no. 23, pp. 2109–2111, Nov. 1996.
[31] N. Gagnon, A. Petosa, and D. A. McNamara, "Research and development on phase-shifting surfaces (PSSs)," *IEEE Antennas Propag. Mag.*, vol. 55, no. 2, pp. 29–48, Apr. 2013.
[32] H. Li, G. Wang, H.-X. Xu, T. Cai, and J. Liang, "X-band phase-gradient metasurface for high-gain lens antenna application," *IEEE Trans. Antennas Propag.*, vol. 63, no. 11, pp. 5144–5149, Nov. 2015.
[33] T. Cai, G.-M. Wang, J.-G. Liang, Y.-Q. Zhuang, and T.-J. Li, "High-performance transmissive meta-surface for *C*-/*X*-band lens antenna application," *IEEE Trans. Antennas Propag.*, vol. 65, no. 7, pp. 3598–3606, Jul. 2017.
[34] K. Liu, Y. Ge, and C. Lin, "A compact wideband high-gain metasurface-lens-corrected conical horn antenna," *IEEE Antennas Wireless Propag. Lett.*, vol. 18, no. 3, pp. 457–461, Mar. 2019.
[35] K. K. Katare, S. Chandravanshi, A. Biswas, and M. J. Akhtar, "Realization of split beam antenna using transmission-type coding metasurface and planar lens," *IEEE Trans. Antennas Propag.*, vol. 67, no. 4, pp. 2074–2084, Apr. 2019.
[36] C. Xue, Q. Lou, and Z. N. Chen, "Broadband double-layered huygens' metasurface lens antenna for 5G millimeter-wave systems," *IEEE Trans. Antennas Propag.*, vol. 68, no. 3, pp. 1468–1476, Mar. 2020.
[37] H. Zhu, S. W. Cheung, and T. I. Yuk, "Enhancing antenna boresight gain using a small metasurface lens: Reduction in half-power beamwidth.," *IEEE Antennas Propag. Mag.*, vol. 58, no. 1, pp. 35–44, Feb. 2016.
[38] A. Dadgarpour, M. Sharifi Sorkherizi, and A. A. Kishk, "Wideband low-loss magnetoelectric dipole antenna for 5G wireless network with gain enhancement using meta lens and gap waveguide technology feeding," *IEEE Trans. Antennas Propag.*, vol. 64, no. 12, pp. 5094–5101, Dec. 2016.
[39] B. Majumder, K. Kandasamy, and K. P. Ray, "A zero index based meta-lens loaded wideband directive antenna combined with reactive impedance surface," *IEEE Access*, vol. 6, pp. 28746–28754, 2018.
[40] J.-J. Liang, G.-L. Huang, J.-N. Zhao, Z.-J. Gao, and T. Yuan, "Wideband phase-gradient metasurface antenna with focused beams," *IEEE Access*, vol. 7, pp. 20767–20772, 2019.
[41] A. K. Singh, M. P. Abegaonkar, and S. K. Koul, "Compact near zero index metasurface lens with high aperture efficiency for antenna radiation characteristic enhancement," *IET Microw., Antennas Propag.*, vol. 13, no. 8, pp. 1248–1254, Jul. 2019.
[42] A. S. Y. Poon, S. O'Driscoll, and T. H. Meng, "Optimal frequency for wireless power transmission into dispersive tissue," *IEEE Trans. Antennas Propag.*, vol. 58, no. 5, pp. 1739–1750, May 2010.
[43] C. A. Balanis, *Antenna Theory: Analysis and Design*, 23rd ed. Hoboken, NJ, USA: Wiley, 2005, pp. 34–35.
[44] R. C. Johnson, H. A. Ecker, and J. S. Hollis, "Determination of far-field antenna patterns from near-field measurements," *Proc. IEEE*, vol. 61, no. 12, pp. 1668–1694, Dec. 1973.

DUY-NINH DANG received the B.S. degree from the School of Electronics and Telecommunications, Hanoi University of Science and Technology, Hanoi, Vietnam, in 2013. He is currently pursuing the integrated master's Ph.D. degree with the Department of Information Communication, Materials, and Chemistry Convergence Technology, Soongsil University, Seoul, South Korea. His current research interests include high-gain antenna, power amplifiers, metamaterials, and wireless power transfer.

CHULHUN SEO (Senior Member, IEEE) received the B.S., M.S., and Ph.D. degrees from Seoul National University, Seoul, South Korea, in 1983, 1985, and 1993, respectively. From 1993 to 1995, he was with the Massachusetts Institute of Technology (MIT), Cambridge, MA, USA, as a Technical Staff Member, where he was also a Visiting Professor, from 1999 to 2001. From 1993 to 1997, he was with Soongsil University, Seoul, as an Assistant Professor, where he was also an Associate Professor, from 1997 to 2004. Since 2004, he has been a Professor of electronic engineering with Soongsil University. He was the IEEE MTT Korea Chapter Chairman, from 2011 to 2014. He is the President of the Korean Institute of Electromagnetic Engineering and Science (KIEES) and the Dean of the Information and Telecommunications College, Soongsil University. He is the Director of the Wireless Power Transfer Research Center, supported by the Korean Government's Ministry of Trade, Industry and Energy; the Metamaterials Research Center, supported by Basic Research Laboratories (BRL) through an NRF Grant funded by Minister of Science, ICT and Future Planning (MSIP); and the Center for Intelligent Biomedical Wireless Power Transfer, supported by the National Research Foundation of Korea (NRF) Grant funded by MSIP. His research interests include wireless technologies, RF power amplifiers, and wireless power transfer using metamaterials.